A NEW METHOD TO PREDICT NON-PROPORTIONALITY FACTORS AND EQUIVALENT STRESSES AND STRAINS IN MULTIAXIAL FATIGUE

Marco Antonio Meggiolaro, meggi@puc-rio.br
Jaime Tupiassú Pinho de Castro, jtcastro@puc-rio.br
Mechanical Engineering Department, PUC-Rio, Brazil

Abstract. *This work presents a new approach to evaluate equivalent stress and strain ranges in non-proportional (NP) histories, called the Moment Of Inertia (MOI) method. The MOI method assumes that the path contour in the stress or strain diagram is a homogeneous wire with unit mass. The center of mass of such wire gives then the mean component of the path, while the moments of inertia of the wire can be used to obtain not only the equivalent stress or strain ranges, but also the non-proportionality factor F_{np}. The MOI method is an alternative to convex hull methods, such as the Minimum Ball or Maximum Prismatic Hull methods, without the need for adjustable parameters or incremental plasticity calculations. The MOI method can deal with an arbitrarily shaped history without losing information about such shape, as opposed to a convex hull method. It is relatively simple, intuitive, and easy to implement and to compute, therefore it should be considered as an alternative engineering tool to deal with NP histories, in special for very long histories where incremental plasticity methods would be too computationally intensive. Experimental results for 15 different multiaxial histories prove the effectiveness of the MOI method to predict the associated fatigue lives, compared to predictions from standard convex hull methods. These experimental results also show that the Minimum Ball method underestimates the equivalent ranges for NP histories, while the Maximum Prismatic Hull method overestimates such range for cross or star-shaped paths.*

Keywords: *multiaxial fatigue; equivalent stress; non-proportionality factor.*

1. INTRODUCTION

Several multiaxial fatigue damage models have been introduced in the literature. All of them require some measure of an equivalent stress or strain range, which may be difficult to obtain for non-proportional (NP) multiaxial histories.

To calculate the fatigue damage induced by a generic NP load history, it is necessary to first project it onto a specified plane at the analyzed point. Then, the projected history must be counted using a multiaxial rainflow algorithm to identify individual cycles. Then, for each cycle, the equivalent stress or strain range is usually computed using the so-called convex hull methods, which try to find circles, ellipses or rectangles that contain the entire path in the 2D case, or hyperspheres, hyperellipsoids or hyperprisms in the generic 5D equivalent stress space. The main convex hull methods are the Minimum Ball (MB) (Dang Van, 1999), Minimum Circumscribed Ellipsoid (MCE) (Freitas et al., 2000), Minimum Volume Ellipsoid (MVE), Minimum F-norm Ellipsoid (MFE) (Gonçalves et al., 2005), Maximum Prismatic Hull (MPH) (Mamiya et al., 2009) and Maximum Volume Prismatic Hull (MVPH).

The MFE and all prismatic hull models are efficient to predict equivalent amplitudes in NP histories. However, all convex hull methods can lead to poor predictions of the mean stresses or strains, if they are assumed as located at the center of the ball, ellipse or prism, as seen in the top example in Fig. 1, which shows a stress or strain path shaped very differently from an ellipse and its MFE hull.

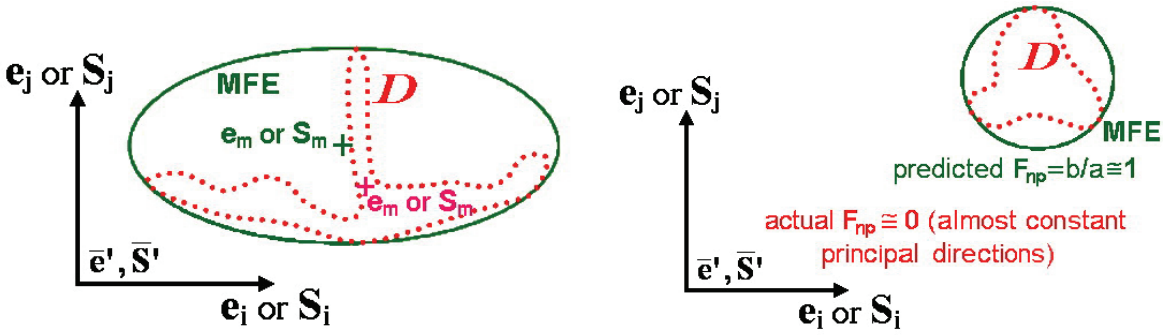

Fig. 1: History path examples showing the inadequacy of convex hull methods (such as the MFE) to predict mean components (left diagram) or the non-proportionality factor F_{np} (right diagram) in deviatoric stress **S** or strain **e** diagrams.

In addition, all convex hull methods can lead to poor predictions of the load history non-proportionality factor F_{np}, if it is measured from the aspect ratio of such hulls. The bottom example in Fig. 1 shows a path that does not encircle the origin of the diagram, while entirely located far away from it. Despite the almost circular shape of the enclosing MFE,

which would suggest $F_{np} \cong 1$, the principal direction in fact varies very little along such path, since the angle between each point in the path and the origin of the 2D diagram varies very little during each cycle – thus, the actual F_{np} should be very small in this example. Note also that the convex hull methods can lead to poor F_{np} preditions even in paths that encircle the origin, in special when the path shape is very different from an ellipse or rectangle, or when the mean value of the path is not located close to the origin.

On the other hand, the Moment Of Inertia (MOI) method, presented in the following sections, is able not only to predict the equivalent stress and strain ranges of NP history paths, such as the better convex hull methods do, but also to estimate well their mean components and the non-proportionality factor F_{np}. Moreover, it can be easier to use.

2. THE MOMENT OF INERTIA (MOI) METHOD

The Moment Of Inertia (MOI) method is useful to calculate alternate and mean components of complex NP load histories. To accomplish that, the history must first be represented in a 2D stress-subspace of the transformed 5D Euclidean stress-space $E_{5\sigma}$ (for stress histories), proposed by Papadopoulos et al. (1997), or its strain-equivalent $E_{5\varepsilon}$ (for strain histories).

Similarly to the convex hull methods, the MOI method should only be applied to 2D histories, involving one normal and one shear stress or strain components (e.g. represented in the $\sigma_x \times \tau_{xy}\sqrt{3}$ or $\varepsilon_x \times \gamma_{xy}\sqrt{3}/(2+2\,\overline{\nu}\,)$ diagrams) or two shear components acting on the same plane (e.g. represented in the $\tau_{xz}\sqrt{3} \times \tau_{xy}\sqrt{3}$ or $\gamma_{xz}\sqrt{3}/(2+2\,\overline{\nu}\,) \times \gamma_{xy}\sqrt{3}/(2+2\,\overline{\nu}\,)$ diagrams). It would lead to significant errors if directly applied to 3D, 4D or 5D load histories, because the MOI method would be calculated on different planes at different points in time (Socie, 1999). Instead, any 3D, 4D or 5D history should be projected onto a candidate plane. Then, the history of the two shear stresses (or strains) acting parallel to the crack plane would be represented in a 2D diagram, where the MOI method would be applied. Thus, only the 2D formulation of the MOI method will be presented here.

The MOI method assumes that the 2D path/domain $\boldsymbol{D}$, represented by a series of points (X, Y) from the stress or strain variations along it, is a homogeneous wire with unit mass. Note that X and Y can have stress or strain units, but they are completely unrelated to the directions x and y usually associated with the material surface. The mean component of $\boldsymbol{D}$ is assumed, in the MOI method, to be located at the center of gravity of this imaginary homogeneous wire shaped as the history path. Such center of gravity is located at the perimeter centroid (X_c, Y_c) of $\boldsymbol{D}$, calculated from contour integrals along the entire path

$$X_c = \frac{1}{p}\cdot\oint X\cdot dp, \quad Y_c = \frac{1}{p}\cdot\oint Y\cdot dp, \quad p = \oint dp \tag{1}$$

where dp is the length of an infinitesimal arc of the path and p is the path perimeter, see Fig. 2.

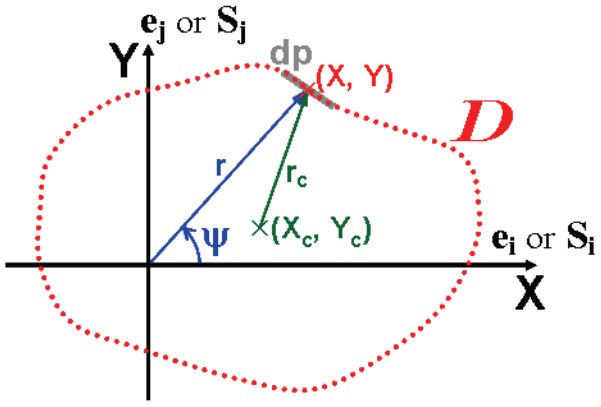

Fig. 2: History path, assumed as a homogeneous wire with unit mass.

Note that this perimeter centroid (PC) is in general different from the area centroid (AC), which is the center of gravity of a uniform density sheet bounded by the shape of a closed path $\boldsymbol{D}$. The PC gives a much more reasonable estimate of the mean component.

The MOI method is so called because it makes use of the mass moments of inertia (MOI) of such homogeneous wire. These moments are first calculated with respect to the origin O of the diagram, assuming the wire has unit mass, resulting in

$$I^O_{XX} = \frac{1}{p}\cdot\oint Y^2\cdot dp, \quad I^O_{YY} = \frac{1}{p}\cdot\oint X^2\cdot dp, \quad I^O_{XY} = -\frac{1}{p}\cdot\oint X\cdot Y\cdot dp \tag{2}$$

Then, the moments of inertia of such unit mass wire, with respect to its center of gravity (X_c, Y_c), are obtained. They are computed from the moments of the path $\boldsymbol{D}$ domain with respect to its perimeter centroid (X_c, Y_c), which are easily obtained from the parallel axis theorem, assuming a unit mass:

$$I_{XX} = I^O_{XX} - Y_c^{\,2}, \quad I_{YY} = I^O_{YY} - X_c^{\,2}, \quad I_{XY} = I^O_{XY} + X_c \cdot Y_c \tag{3}$$

The MOI method assumes that the deviatoric stress or strain ranges, $\Delta S \equiv \Delta\sigma_{Mises}$ or $\Delta e \equiv \Delta\varepsilon_{Mises}$, depend on the mass moment of inertia I_{ZZ} with respect to the perimeter centroid, perpendicular to the X-Y plane. This is physically sound, since history paths further away from the PC will contribute more to the effective range and amplitude, which is coherent with the fact that wire segments further away from the center of gravity of an imaginary homogeneous wire contribute more to its MOI. From the perpendicular axis theorem, which states that $I_{ZZ} = I_{XX} + I_{YY}$, and from a dimensional analysis, it is found that

$$\frac{\Delta\sigma_{Mises}}{2} \text{ or } \frac{\Delta\varepsilon_{Mises}}{2} = \sqrt{3 \cdot I_{ZZ}} = \sqrt{3 \cdot (I_{XX} + I_{YY})} \tag{4}$$

The factor $\sqrt{3}$ is introduced to guarantee that a proportional loading path, represented by a straight segment with length L (Fig. 3) and unit mass $m = 1$, will result in the expected range $\Delta\sigma_{Mises}$ or $\Delta\varepsilon_{Mises}$ equal to L:

$$I_{zz} = \frac{m \cdot L^2}{12} \Rightarrow \Delta\sigma_{Mises} \text{ or } \Delta\varepsilon_{Mises} = 2 \cdot \sqrt{3 \cdot \frac{1 \cdot L^2}{12}} = L \tag{5}$$

since the MOI of a straight wire with respect to its centroid is $m \cdot L^2/12$.

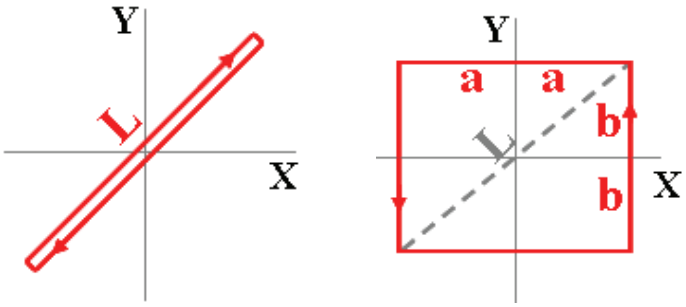

Fig. 3: Proportional and rectangular history paths.

Note that the above definitions are coherent, since they are independent of the orientation of the X-Y system because $I_{XX} + I_{YY}$ is an invariant, equal to the sum of the principal MOI $I_1 + I_2$ of the homogeneous wire.

Let's now calculate, using the MOI method, the equivalent range of a history $X \times Y \equiv e_1 \times e_3 \equiv \varepsilon_x \times \gamma_{xy}\sqrt{3}/(2+2\bar{\nu})$ defined by the rectangular path from Fig. 3, centered at the origin. Imagining such path as a homogeneous wire with unit mass, then its perimeter is $p = 4a + 4b$, while each of the two horizontal rods has mass $m_a = 2a/p$ and each vertical rod has $m_b = 2b/p$ (the sum of the masses of all 4 rods is therefore equal to $2 \cdot (2a+2b)/p = 1$, as required by the MOI method). The longest chord of the path is the rectangle diagonal $L = 2 \cdot (a^2 + b^2)^{1/2}$. From the path symmetry, the PC (X_c, Y_c) is located at the origin, thus

$$I_{xx} = I^O_{xx} = 2 \cdot (m_a b^2 + m_b b^2 / 3), \quad I_{yy} = I^O_{yy} = 2 \cdot (m_b a^2 + m_a a^2 / 3) \tag{6}$$

$$\Delta\varepsilon_{Mises} = 2 \cdot \sqrt{3 \cdot \frac{2}{p} \cdot \left[2ab^2 + \frac{2b^3}{3} + 2ba^2 + \frac{2a^3}{3} \right]} = 2 \cdot (a + b) \tag{7}$$

which is exactly the value predicted by the MPH method, resulting in a ratio

$$\lambda_{MOI} \equiv \frac{\Delta\varepsilon_{Mises}}{L} = \frac{2 \cdot (a+b)}{2 \cdot \sqrt{a^2 + b^2}} = \frac{a+b}{\sqrt{a^2 + b^2}} \tag{8}$$

The MOI method is simple to calculate, in special for polygonal histories. The moments of curved histories are also easy to calculate from fine polygonal discretizations. In addition, the MOI method can make use of classical mass moment of inertia tables, or even CAD programs applied to arbitrarily shaped homogeneous wires, to calculate I_{XX}, I_{YY}, I_{XY} and I_{ZZ}.

To use the MOI approach in polygonal load history paths, it is enough to combine the expression for the moment of inertia of an inclined straight wire and the parallel axis theorem. If each side i of the polygon has length Δp_i, centered at (X_{ci}, Y_{ci}), and making an angle ψ_i with respect to the horizontal (see Fig. 4), then the perimeter centroid PC and the MOI expressions with respect to the origin are obtained from

$$p = \sum_i \Delta p_i, \quad X_c = \frac{1}{p} \cdot \sum_i X_{ci} \cdot \Delta p_i, \quad Y_c = \frac{1}{p} \cdot \sum_i Y_{ci} \cdot \Delta p_i$$
$$I^O_{XX} = \frac{1}{p} \cdot \sum_i \left(\frac{\Delta p_i^2}{12} \sin^2 \psi_i + Y_{ci}^2 \right) \cdot \Delta p_i, \quad I^O_{YY} = \frac{1}{p} \cdot \sum_i \left(\frac{\Delta p_i^2}{12} \cos^2 \psi_i + X_{ci}^2 \right) \cdot \Delta p_i, \tag{9}$$
$$I^O_{XY} = -\frac{1}{p} \cdot \sum_i \left(\frac{\Delta p_i^2}{12} \sin\psi_i \cos\psi_i + X_{ci} Y_{ci} \right) \cdot \Delta p_i$$

The MOI with respect to the PC is then calculated from Eq. (3).

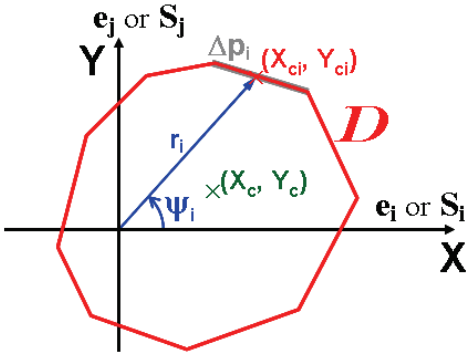

Fig. 4: Application of the MOI method for polygonal history paths.

For instance, let's use the above equations for polygonal paths to calculate the equivalent range of a history $e_1 \times e_3$ defined by the square path from Fig. 5, centered at the origin. Applying the above equations for the 4 sides $\Delta p_i = a$, then

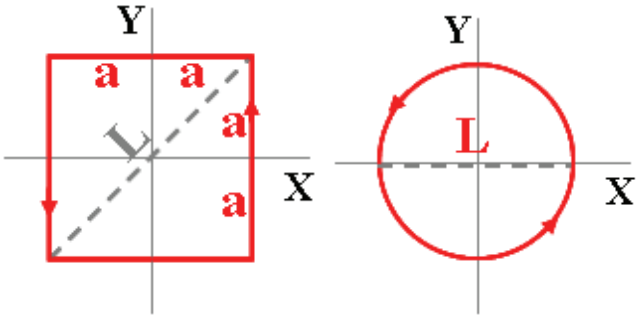

Fig. 5: Square and circular history paths.

$$p = 8a, \quad X_c = \frac{1}{8a} \cdot (a + 0 - a + 0) \cdot 2a = 0, \quad Y_c = \frac{1}{8a} \cdot (0 + a + 0 - a) \cdot 2a = 0,$$
$$I^O_{XX} = \frac{1}{8a} \cdot \left(\frac{4a^2}{12} + a^2 + \frac{4a^2}{12} + a^2 \right) \cdot 2a = \frac{4a^2}{6} = I_{XX} + Y_c^2 = I_{XX}, \tag{10}$$
$$I^O_{YY} = \frac{1}{8a} \cdot \left(a^2 + \frac{4a^2}{12} + a^2 + \frac{4a^2}{12} \right) \cdot 2a = \frac{4a^2}{6} = I_{YY} + X_c^2 = I_{YY},$$
$$I^O_{XY} = -\frac{1}{8a} \cdot (0 + 0 + 0 + 0) \cdot 2a = 0, \quad I_{ZZ} = I_{XX} + I_{YY} = \frac{4a^2}{3}$$
$$\Delta\varepsilon_{Mises} = 2 \cdot \sqrt{3 \cdot \frac{4a^2}{3}} = 4a \quad \Rightarrow \quad \lambda_{MOI} \equiv \frac{\Delta\varepsilon_{Mises}}{L} = \frac{4a}{2a\sqrt{2}} = \sqrt{2} \tag{11}$$

which agrees with the value predicted by the MPH method.

For a circular path with diameter L (Fig. 5), centered at the origin, the equivalent range is easily calculated from the expression of the moment of inertia $I_{ZZ} = m \cdot (L/2)^2$ of a circular ring with unit mass $m = 1$, resulting in

$$\Delta\sigma_{Mises} \text{ or } \Delta\varepsilon_{Mises} = 2 \cdot \sqrt{3 \cdot I_{ZZ}} = 2 \cdot \sqrt{3 \cdot \frac{1 \cdot L^2}{4}} = L\sqrt{3} \tag{12}$$

The above result is different from the ones obtained from most convex hull methods, which would predict a range $L\sqrt{2}$ in this case. But the higher value $L\sqrt{3}$ is physically reasonable. A square path with diagonal L (which is its longest chord) results in an equivalent range $L\sqrt{2}$ according to most convex hull methods. It is reasonable to assume that a circular path circumscribing such square, which would describe a *57%* larger area in the diagram, should result in a somewhat larger effective stress or strain range, e.g. *22.5%* larger as predicted by the MOI method. The literature has shown that both circular and square paths with same longest chord L result in not too different lives, but certainly not in the exact same lives, as most convex hull methods would suggest. So, the $L\sqrt{3}$ prediction by the MOI method might be better than the convex hull predictions $L\sqrt{2}$ for circular paths.

The MOI method, despite physically reasonable and agreeing in most cases with the best convex hull methods, is not a physical law. So, it is possible to include a fitting exponent β ($\beta > 0$) to better reproduce experimental data

$$\frac{\Delta\sigma_{Mises}}{2} \text{ or } \frac{\Delta\varepsilon_{Mises}}{2} = \left[\sqrt{3 \cdot (I_{XX} + I_{YY})}\right]^{\beta} \cdot L^{1-\beta} = \left[\sqrt{3 \cdot I_{ZZ}}\right]^{\beta} \cdot L^{1-\beta} \tag{13}$$

where L is the length of the longest chord of the history. The originally proposed MOI equation represents the case $\beta = 1$. If, for instance, the equivalent (or Mises) range of a circular path is measured as a value $L \cdot \lambda_{meas}$ instead of $L\sqrt{3}$ (from the original MOI method) or $L\sqrt{2}$ (from most convex hull methods), then a fitting exponent $\beta = log(\lambda_{meas})/log(\sqrt{3})$ could be used in such generalized MOI method.

3. CALCULATION OF THE NON-PROPORTIONALITY FACTOR F_{NP}

To account for NP hardening effects, it is necessary to correctly evaluate the non-proportionality factor F_{np}. The NP factor F_{np} can be estimated from the load history path. However, as previously shown, convex hulls are not a good option to estimate F_{np}. For instance, a path formed by a straight line that does not cross the origin of the diagram can result in a large variation of the principal directions, resulting in $F_{np} > 0$, however any convex hull method would predict that $F_{np} = 0$ for a straight line.

Several methods have been proposed to estimate F_{np}. Kanazawa et al. (1979) estimated F_{np} as a rotation factor, defined by the ratio between the shear strain range at 45° from the maximum shear plane and the maximum shear strain range. This factor correctly tends to the limits $F_{np} = 0$ for proportional loadings and $F_{np} = 1$ for 90° out-of-phase strain histories, assuming the relation $\gamma_a = (1+\bar{\nu}) \cdot \varepsilon_a$ between strain amplitudes for Case A cracks (Socie, 1999). But it fails to correctly compute F_{np} for more complex histories. Other F_{np} estimates can be found in (Doong and Socie, 1991).

Itoh (Kida et al., 1997) estimated F_{np} using a contour integral definition along the path. This Itoh-Socie method searches for the direction of maximum strain in the path, and then it performs an integral average along the entire path of the absolute value of the strain components perpendicular to such direction. The ratio between this strain average and the maximum strain is used to estimate F_{np}. A reasonable agreement between the predictions from Itoh-Socie's method and experimental data indicates that an integral definition of F_{np} seems to work very well. Since the presented MOI method also involves integrals in its definitions, it might be a good option as well to compute F_{np}, as described next.

A variation of the Moment Of Inertia (MOI) method is now proposed to evaluate the non-proportionality factor F_{np}. To accomplish that, consider a projection from the 6D deviatoric stress space onto a 5D stress-subspace $E_{5\sigma}$* slightly different from the one proposed by Papadopoulos (1997):

$$\begin{cases} \bar{S}^* \equiv \left[S_1^* \quad S_2^* \quad S_3^* \quad S_4^* \quad S_5^* \right]^T \\ S_1^* \equiv \dfrac{\sigma_x - \sigma_y}{2}\sqrt{3} = \dfrac{S_x - S_y}{2}\sqrt{3}, \quad S_2^* \equiv \sigma_z - \dfrac{\sigma_x}{2} - \dfrac{\sigma_y}{2} = \dfrac{3}{2} S_z \\ S_3^* \equiv \tau_{xy}\sqrt{3}, \quad S_4^* \equiv \tau_{xz}\sqrt{3}, \quad S_5^* \equiv \tau_{yz}\sqrt{3} \end{cases} \tag{14}$$

as well as a slightly different projection $E_{5\varepsilon}$* from the 6D deviatoric strain-space:

$$\begin{cases} \bar{e}^* \equiv \left[e_1^* \quad e_2^* \quad e_3^* \quad e_4^* \quad e_5^* \right]^T \\ e_1^* \equiv \dfrac{e_x - e_y}{2 \cdot (1+\bar{\nu})}\sqrt{3} = \dfrac{\varepsilon_x - \varepsilon_y}{2 \cdot (1+\bar{\nu})}\sqrt{3}, \quad e_2^* \equiv \dfrac{3}{2} \cdot \dfrac{e_z}{1+\bar{\nu}} = \dfrac{2\varepsilon_z - \varepsilon_x - \varepsilon_y}{2 \cdot (1+\bar{\nu})}, \\ e_3^* \equiv \dfrac{\gamma_{xy}\sqrt{3}}{2 \cdot (1+\bar{\nu})}, \quad e_4^* \equiv \dfrac{\gamma_{xz}\sqrt{3}}{2 \cdot (1+\bar{\nu})}, \quad e_5^* \equiv \dfrac{\gamma_{yz}\sqrt{3}}{2 \cdot (1+\bar{\nu})} \end{cases} \tag{15}$$

Both projections above have the same properties as the projections proposed by Papadopoulos (1997). The reason for picking these new sub-spaces is that using them the principal direction θ_p with respect to the x axis can now be represented by

$$tan\,2\theta_p = \frac{2\tau_{xy}}{\sigma_x - \sigma_y} = \frac{S_3^*}{S_1^*} \quad \text{and} \quad tan\,2\theta_p = \frac{\gamma_{xy}}{\varepsilon_x - \varepsilon_y} = \frac{e_3^*}{e_1^*} \tag{16}$$

Therefore, the angle $\psi \equiv 2\theta_p$ of each state in the $S_1 \times S_3$ diagram is equal to each angle ψ measured from the center of successive Mohr circles, which in turn is equal to twice each principal direction θ_p. Therefore, the $E_{5\sigma}$* and $E_{5\varepsilon}$* subspaces provide a graphical way to visualize the intensity of the stresses or strains at each principal direction $\theta_p \equiv \psi/2$ (for normal vs. shear diagrams) or $\theta_p \equiv \psi$ (for shear vs. shear diagrams), since the Mises stress or strain is the magnitude of the vector r.

Thus, to calculate the directions suffering larger stress or strain magnitudes, the load history path $\boldsymbol{D}$ can be imagined as a homogeneous wire with unit mass, as it was assumed before to calculate the Mises ranges. This is physically sound, since the mass moments of inertia I_{XX}^* and I_{YY}^* of such wire with respect to the origin in the horizontal (X) and vertical (Y) directions are a measure of how much the path stretches in the Y and X directions, respectively.

If the path crosses more than once some direction ψ, then it is reasonable to assume that the point with maximum magnitude r among them is the one that better represents the contribution of the Mises stresses or strains in this direction. This means that the MOI equations to compute F_{np} must be evaluated only for the enclosing hull (which is not necessarily convex) defined by the outer perimeter of the entire history path. Note that this hull must be computed for the entire history (since the specimen was virgin up to a certain point in time) to be able to account for all non-proportional hardening suffered along the specimen life until now (the previously presented MOI method for the range and mean calculations, on the other hand, do not make use of any hull, and they are computed for each rainflow-counted cycle, not for the entire history). If p is the perimeter of such enclosing hull, then the moments of inertia of the hull are obtained from

$$I_{XX}^* = \frac{1}{p}\cdot\oint Y^2\cdot dp, \quad I_{YY}^* = \frac{1}{p}\cdot\oint X^2\cdot dp, \quad I_{XY}^* = -\frac{1}{p}\cdot\oint X\cdot Y\cdot dp, \quad p = \oint dp \tag{17}$$

The MOI I_e* in the direction ψ_e of the maximum projected deviatoric strain e_{max}* from the history is then

$$I_e^* = \frac{I_{XX}^* + I_{YY}^*}{2} + \frac{I_{XX}^* - I_{YY}^*}{2}cos\,2\psi_e + I_{XY}^*\,sin\,2\psi_e \tag{18}$$

The NP factor F_{np} is then defined in the MOI method as

$$F_{np} = \sqrt{2\cdot I_e^*}\,/\,e_{max}^* \tag{19}$$

4. COMPARISONS AMONG THE EFFECTIVE RANGE PREDICTIONS

The convex hull and MOI predictions of effective ranges are now compared to experimental measurements from Itoh (Kida et al., 1997) in a 304 stainless steel. Thirteen periodic histories are studied, represented by the block loadings shown in Fig. 6 for Cases 0 through 12. In addition, two histories from Shamsaei et al. (2010) are considered, named FRI and FRR. For each block of the FRI loading, 360 cycles are applied to the specimen, with principal directions varying in 1° increments. For the FRR loading, the principal direction of each of the 360 cycles is randomly chosen, leading to abrupt changes in principal directions, see Fig. 6.

Note that most loadings from Fig. 6 consider 1 cycle per block, except for Cases 1 through 4, which consider 2 cycles per block, and the FRI and FRR loadings, with 360 cycles per block. The number of cycles in each block can be deterministically obtained using a modification of the Wang Brown rainflow algorithm.

The effective range predictions are now evaluated for the 13 histories from Itoh-Socie. The effective ranges are use predict the multiaxial fatigue lives for each history, which are then compared to experimental measurements from Kida et al. (1997). For the damage calculation, the properties of the 304 stainless steel used by Itoh et al. must be known:

$$\varepsilon = \frac{\sigma}{E} + \left(\frac{\sigma}{1754}\right)^{1/0.276}, \; E = 197{,}000\,MPa, \quad b = -0.0886, \quad c = -0.303$$
$$(\sigma_{max}\frac{\Delta\varepsilon}{2})_{max} = \frac{757^2}{E}(2N)^{2b} + 30.5\cdot(2N)^{b+c} \tag{20}$$

As it can be seen in Eq. (20), Ramberg-Osgood and the Smith-Watson-Topper (SWT) damage model are used in a critical plane approach, generating the results from Table 1 according to the MOI, MB and MPH methods. Note that the

MOI method considers 2 cycles per block for Cases 1 through 4 (marked with an * in the Table), as obtained by a modified Wang Brown multiaxial rainflow count.

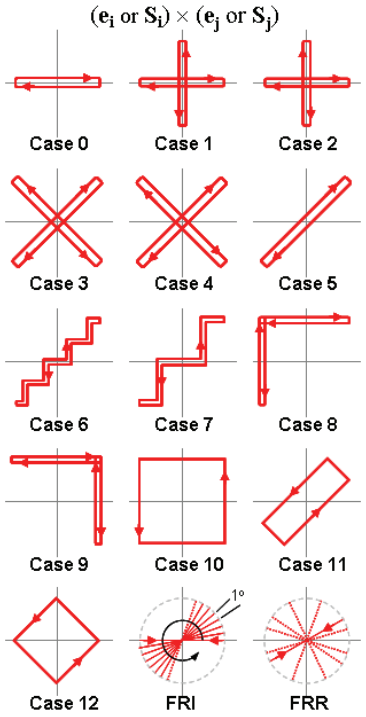

Fig. 6: History paths used in the experimental validation of the F_{np} and equivalent range predictions.

Table 1: Predictions of $\lambda = \Delta\sigma_{Mises}/L$ or $\lambda = \Delta\varepsilon_{Mises}/L$ used to calculate the equivalent amplitudes, according to the MOI, MB and MPH methods.

path / λ	MOI	MB	MPH
Case 0	1	1	1
Case 1	1*	1	√2
Case 2	1*	1	√2
Case 3	1*	1	√2
Case 4	1*	1	√2
Case 5	1	1	1
Case 6	1.01	1	1.03
Case 7	1.03	1	1.06
Case 8	1.12	1	1.14
Case 9	1.12	1	1.14
Case 10	√2	1	√2
Case 11	1.263	1	1.263
Case 12	1.411	1	1.411

as if 90° out of phase

good predictions

good predictions

as if proportional

It can be seen from Table 1 that the MOI method predicts that Cases 0 through 5 are proportional, since their ratio $\lambda_{MOI} = 1$. This is reasonable, because the star and cross shaped histories from Cases 1-4 are indeed the combination of 2 perpendicular proportional paths. The MPH generates bad predictions in this case, since such convex hull method wouldn't be able to distinguish between a cross shaped and a circular history, wrongfully predicting $\lambda_{MPH} = \sqrt{2}$.

For Cases 5-12, the MOI method also predicts λ very well, agreeing with the MPH predictions. However, the MB method implicitly assumes that all cases are proportional, since their $\lambda_{MB} = 1$, leading to poor predictions for Cases 8-12.

From the equivalent amplitudes $\lambda \cdot L$ calculated above, the fatigue lives N (in cycles) can be predicted from these methods, and compared to experimental measurements from Kida et al. (1997), see Table 2 and Fig. 7. Note that the SWT model is used here in the plane that maximizes the damage parameter $\sigma_{max} \cdot \Delta\varepsilon/2$, not in the direction of maximum $\Delta\varepsilon/2$.

As expected from the quality of the λ predictions, the MOI method results in quite good life predictions in all studied histories, all estimated within only 20% from the experimental results. Note that these are not curve fittings, they are true predictions made using the MOI method (together with SWT) without any adjustable parameter, since both β and β^* exponents from the generalized MOI method were assumed as their default (original) values *1.0*. The MPH method, on the other hand, gives poor life predictions for Cases 1-4, since it wrongfully assumes (through $\lambda_{MPH} = \sqrt{2}$) that these cross or star-shaped histories are 90° out-of-phase, instead of being proportional. And the MB method results in non-conservative predictions in Cases 8-12, since it wrongfully assumes (through $\lambda_{MB} = 1$) that these paths are proportional.

Table 2: Fatigue life predictions N (in cycles) using the SWT damage model and the MOI, MB and MPH methods. Note that Cases 1-4 consider 2 cycles per block, e.g. the measured life for Case 1 was 1,400 blocks and thus 2,800 cycles.

path / N	experim.	MOI	MB	MPH
Case 0	7100	7085	7085	7085
Case 1	2800	3379	3379	1150
Case 2	4200	4462	4462	1504
Case 3	820	640	640	229
Case 4	900	858	858	304
Case 5	3200	3557	3557	3557
Case 6	2600	2332	2393	2177
Case 7	1700	1590	1751	1453
Case 8	470	604	856	572
Case 9	660	604	856	572
Case 10	320	329	949	329
Case 11	1200	1073	2241	1073
Case 12	710	689	2023	689

as if 90° out of phase

as if proportional

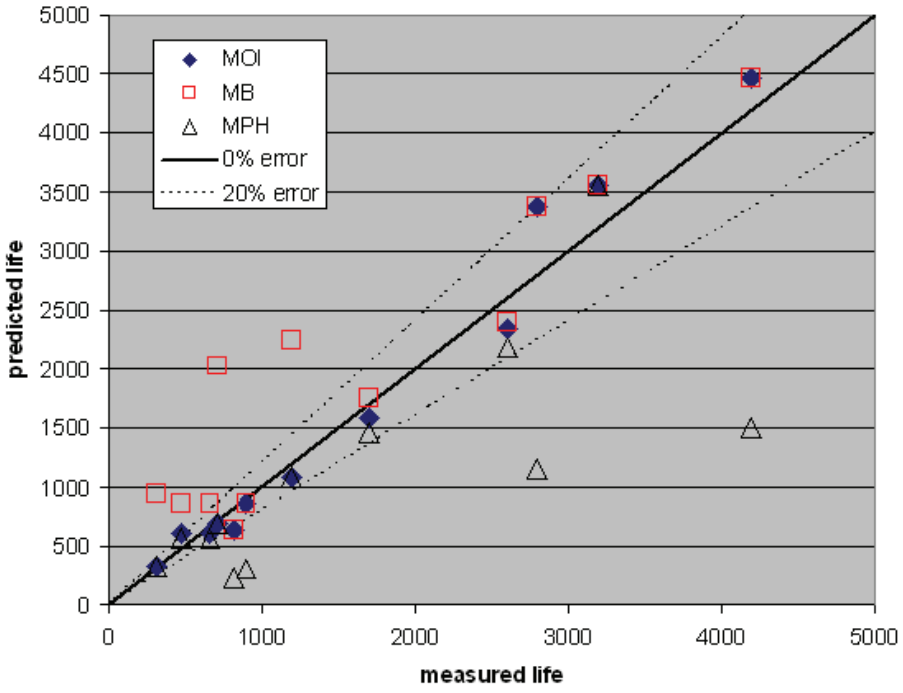

Fig. 7: Measured and predicted fatigue lives using SWT and the MOI, MB and MPH methods, for a 304 stainless steel.

5. CONCLUSIONS

The MOI method is an alternative to convex hull methods to obtain equivalent amplitude/range and mean components of NP histories, in addition to efficiently predicting F_{np}, without the need for adjustable parameters or incremental plasticity calculations. From a philosophical point of view, it is difficult to justify that a convex hull that does not represent well F_{np} or the mean component of a path could be used to calculate the equivalent stress or strain ranges/amplitudes. This is even more difficult to justify when the path has a very odd shape. The MOI method, on the other hand, can calculate all these quantities using the same concepts, showing a much better coherence than any convex hull methods. And, since it accounts for the contribution of every single segment of the path, the MOI method can deal with an arbitrarily shaped history without losing information about such shape, as a convex hull method would.

Experimental results demonstrated the effectiveness of the MOI method for all studied cases. It was also found that the Minimum Ball method underestimates the effective ranges for NP histories, while the Maximum Prismatic Hull method (as well as most convex hull methods such as the MVPH, MPHLC, MPHCC and MFE) overestimate such range for cross or star-shaped paths.

6. ACKNOWLEDGEMENTS

CNPq has provided research scholarships for the authors.

7. REFERENCES

Dang Van, K., Papadopoulos, I.V., High-Cycle Metal Fatigue. Springer 1999.

Doong, S.H., Socie, D.F., Constitutive modelling of metals under nonproportional cyclic loading, J. Eng. Mater. Technol. v.113, pp.23–30, 1991.

Freitas, M., Li, B., Santos, J.L.T., Multiaxial Fatigue and Deformation: Testing and Prediction, ASTM STP 1387, 2000.

Gonçalves, C.A., Araújo, J.A., Mamiya, E.N., Multiaxial fatigue: a stress based criterion for hard metals, International Journal of Fatigue v.27, pp.177-187, 2005.

Kanazawa, K., Miller, K., Brown, M., Cyclic deformation of 1% Cr-Mo-V steel under out-of-phase loads, Fatigue Fract. Eng. Mater. Struct. v.2, pp.217–228, 1979.

Kida, S., Itoh, T., Sakane, M., Ohnami, M., Socie, D.F., Dislocation structure and non-proportional hardening of type 304 stainless steel, Fatigue and Fracture of Engineering Materials and Structures, v.20, n.10, pp.1375-1386, 1997.

Mamiya, E.N., Araújo, J.A., Castro, F.C., Prismatic hull: A new measure of shear stress amplitude in multiaxial high cycle fatigue, International Journal of Fatigue, v.31, pp.1144-1153, 2009.

Papadopoulos, I.V., Davoli, P., Gorla, C., Filippini, M., Bernasconi, A., "A comparative study of multiaxial high-cycle fatigue criteria for metals", Int. Journal of Fatigue v.19, pp.219–235, 1997.

Shamsaei, N., Fatemi, A., Socie, D.F., Multiaxial cyclic deformation and non-proportional hardening employing discriminating load paths, International Journal of Plasticity, v.26, n.12, pp.1680-1701, 2010.

Socie, D.F., Marquis, G.B. Multiaxial Fatigue, SAE 1999.

8. RESPONSIBILITY NOTICE

The authors are the only responsible for the printed material included in this paper.